

화학제적제어계통 정화이온교환기의
파과곡선 특성 분석

김유환, 이상섭, 김은기

원자로설계개발단, 한국전력기술(주)

**A Study on the Breakthrough Characteristics
of CVCS Purification Ion Exchanger**

Y.H.Kim, S.S.Lee and E.K.Kim
NSSS Engineering & Development, KOPEC

1. Introduction

Ion exchange is a very efficient technique for treating radioactive fluids at nuclear power plants[1]. In Ulchin Nuclear Power Plant Units 3 & 4(UCN 3&4), two purification ion exchangers(PIXs) contain mixed bed resins and are provided with the necessary connections to replace resins by sluicing. Each ion exchanger is designed to pass the reactor coolant letdown flow and is identical in design. One purification ion exchanger continuously removes impurities and radionuclides from the reactor coolant letdown flows. The other ion exchanger is used intermittently to control the lithium concentration in the reactor coolant.

The purpose of this paper is to evaluate the Chemical and Volume Control System(CVCS) PIX performance by analyzing the effect of CVCS letdown flowrate and IX resin particle size on the breakthrough characteristics. The characteristics are based on the breakthrough time and exhaustion time for sulfate ion because sulfates are supposed to cause the primary side cracking of alloy 600 material and turbine blades corrosion of Pressurized Water Reactor(PWR).

2. Mathematical equations

2-1 Diffusion and adsorption modelling of breakthrough curve

A brief description of the model[2] is given below. For this process, the kinetic behavior is determined by the rate-controlling mechanism. Three commonly encountered mechanisms are (1) transfer of solute from solution to resin surface, (2) adsorption of solute at solid surface, and (3) diffusion of adsorbed solute through the resin.

The combined surface film and internal solid diffusion are assumed in the system for this study. In addition, this model assumes the followings : (1) constant liquid-film resistance during operation, (2) constant diffusion coefficient of solute through resin, (3) insignificant longitudinal diffusion, (4) presence of only axial flow through resin bed, (5)

uniform bed porosity, (6) no radial variation of concentration in liquid and solid phases, and (7) perfect spherical particles of uniform size.

2-1-1. Mass balance

For the differential PIX column section ΔZ shown in Fig.1[3], the general mass balance of reactor coolant nuclide A in the axial direction is

$$(\text{rate of } A \text{ in}) - (\text{rate of } A \text{ out}) = (\text{rate of } A \text{ accumulation})$$

Since the impurities are transported through the differential element by both diffusion and bulk flow, and they are accumulated in the ion exchange resin particles and interstices, the mass balance becomes

$$\begin{aligned} & \epsilon S \left[-D_s \frac{\partial C_A}{\partial Z} + C_A V_z \right]_{z,t} - \epsilon S \left[-D_s \frac{\partial C_A}{\partial Z} + C_A V_z \right]_{z+\Delta z,t} \\ & = [S \Delta Z \epsilon \frac{\partial C_A}{\partial t}]_z + [S \Delta Z (1 - \epsilon) \frac{\partial C_{As}}{\partial t}]_z \end{aligned} \quad (1)$$

where,

S = cross-sectional area of the PIX column,

ϵ = void fraction in the adsorption bed of PIX,

D_s = effective axial diffusion coefficient of A,

V_z = linear flow velocity (cm/sec),

Z = distance measured from input face of bed (cm),

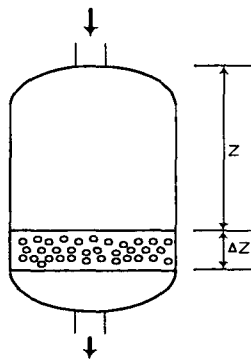
C_A = concentration of nuclide A in the fluid phase (meq/cc),

C_{As} = average concentration of nuclide A in the solid phase of resin (meq/cc)

Rearranging the above equation, and dividing both sides by $\epsilon S \Delta Z$, we obtain

$$\left(D_s \frac{\partial^2 C_A}{\partial Z^2} \right)_t - \left(V_z \frac{\partial C_A}{\partial Z} \right)_t = \left(\frac{\partial C_A}{\partial t} \right)_z + \left(\frac{1 - \epsilon}{\epsilon} \frac{\partial C_{As}}{\partial t} \right)_z \quad (2)$$

Letdown Flow(In), C_{A_0} , V_z



Letdown Flow(Out), C_A , V_z

Fig. 1. Mass balance of PIX in the axial direction.

Neglecting axial diffusion in Eq.(2) gives

$$-\frac{\varepsilon}{1-\varepsilon} V_z \left(\frac{\partial C_A}{\partial Z} \right)_t - \frac{\varepsilon}{1-\varepsilon} \left(\frac{\partial C_A}{\partial t} \right)_z = \left(\frac{\partial C_{As}}{\partial t} \right)_z \quad (3)$$

Introducing $\rho_s = \frac{\rho_b}{1-\varepsilon}$, $q_A = \frac{C_{As}}{\rho_s}$ in Eq.(3) and rearranging the equation,

$$-\frac{\varepsilon}{\rho_b} V_z \left(\frac{\partial C_A}{\partial Z} \right)_t - \frac{\varepsilon}{\rho_b} \left(\frac{\partial C_A}{\partial t} \right)_z = \left(\frac{\partial q_A}{\partial t} \right)_z \quad (4)$$

If the fluid content of the bed is small compared to the total volume of fluid throughput, the second term in Eq.(4) may be neglected[4], as indicated by

$$-\frac{\varepsilon}{\rho_b} V_z \left(\frac{\partial C_A}{\partial Z} \right)_t = \left(\frac{\partial q_A}{\partial t} \right)_z \quad (5)$$

The equation is simplified to

$$\therefore \frac{\partial C_A}{\partial x} + \frac{\partial q_A}{\partial \theta} = 0 \quad (6)$$

$$\text{where, } x = \frac{Z \rho_b}{\varepsilon V_z} \text{ and } \theta = t - \frac{Z}{V_z}$$

The following boundary conditions are used.

$$\text{B.C. 1: } C_A = C_{A_0} \quad \text{at } x = 0 \text{ for all } \theta \quad (7)$$

$$\text{B.C. 2: } q_A = 0 \quad \text{at } \theta = 0 \text{ for all } x \quad (8)$$

The mass transfer through the stagnant film surrounding the resin particle can be expressed as

$$\frac{\partial q_A}{\partial \theta} = \frac{K_f}{\rho_b} (C_A - C_{Ai}) \quad (9)$$

where, K_f = fluid-phase mass transfer coefficient

The diffusion inside a spherical resin particle can be expressed as

$$\frac{\partial q_i}{\partial \theta} = D_s \nabla^2 q_i = \frac{D_s}{r^2} \frac{\partial}{\partial r} \left(r^2 \frac{\partial q_i}{\partial r} \right) = D_s \left[\frac{\partial^2 q_i}{\partial r^2} + \frac{2}{r} \frac{\partial q_i}{\partial r} \right] \quad (10)$$

Average concentration in the resin is indicated by the internal concentration at radius r as

$$q_A = \frac{\int_0^R q_i r^2 dr}{\int_0^R r^2 dr} = \frac{3}{R^3} \int_0^R q_i r^2 dr \quad (11)$$

The following boundary conditions are used.

$$\text{B.C. 1: } q_i = 0 \quad \text{at } \theta = 0 \text{ for all } \chi, r \quad (12)$$

$$\text{B.C. 2: } \frac{\partial q_i}{\partial r} = 0 \quad \text{at } r = 0 \text{ for all } \chi, \theta \quad (13)$$

$$\text{B.C. 3: } q_i = q_s = K_D C_i \text{ at } r = R \quad (14)$$

The following linear isotherm relationship is assumed in this work :

$$q_s = K_D C \quad (15)$$

where, K_D = the distribution coefficient

2-1-2. Numerical solutions

To obtain transient response, the simultaneous partial differential Eqs. (6)~(15) are solved. Analytical solutions for this model are given as follows :

$$\text{If } \frac{\nu}{X} \cong 0,$$

$$\frac{C_A}{C_{A_s}} = \frac{1}{2} \left\{ 1 + \operatorname{erf} \frac{\left(\frac{3Y}{2X} \right) - 1}{\sqrt{5X}} \right\} \quad (15)$$

$$\text{where, } X = \frac{3D_s K_D \rho_s Z}{m V_z R^2} \text{ (bed-length parameter)}$$

$$Y = \frac{2D_s}{R^2} \left(t - \frac{Z}{V_z} \right) \text{ (contact-time parameter)}$$

$$\nu = \frac{D_s K_D \rho_s}{R K_f} \text{ (film-resistance parameter)}$$

$$m = \frac{\varepsilon}{(1 - \varepsilon)}$$

R = radius of the resin particle

3. Results and discussion

3-1 Operating and analytical parameters

The breakthrough curves are predicted based on the operating and analytical parameters of the PIX. Table 1 lists the operating and analytical parameters of the PIX of UCN 3&4. The mass transfer of sulfate ion in fresh ion exchange resin is cited per Ref. 6. The diffusivity value for sulfate ion is available in Ref. 7. Also, the distribution

coefficient for ion exchange resin is available in Ref. 8.

Table 1. Operating and analytical parameters of the PIX of UCN 3&4

Operating conditions	Values[5]	Properties of PIX resin	Values[6]	Analytical parameters[7-9]	Values
Operating temperature, °C	49	True density (ρ_s)(wet), g/cm ³	1.1	Diffusivity(D_s),cm ² /s	1×10^{-5}
Operating pressure, kg/cm ² a	5.25	Resin particle Sizes, mm	0.4(Min.)* 0.55(Effe.) 1.2(Max.)	Mass transfer coefficient(K_p), cm/s	2×10^{-2}
Bed depth(Z), cm	109.22	Void fraction(ϵ), %	32.7	Distribution coefficient(K_D),cm ³ /g	1.5×10^4
Velocity(V_z), cm/s	0.21118(Min.) 0.5310(Nor.) 0.9533(Max.)	Supplier	Rohm & Haas	-	-

*For nuclear grade, the minimum resin particle size is 0.2 mm.

3-2 Breakthrough behavior

3-2-1. Effect of CVCS letdown flowrate

The CVCS letdown flowrates vary in the range of 30 gpm through 135 gpm continuously during normal operation of UCN 3&4. As the flowrate increases from 30 gpm to 75 and 135 gpm, the slope of breakthrough curve for sulfate becomes steeper and the effluent breakthrough trace appears rapidly as shown in Fig.2. As the letdown flowrate increases, the ion exchange time between ion exchange resin and impurity ions is reduced. Therefore, the impurities of nuclide can be effluted from the ion exchange resin bed without completing the ion exchange.

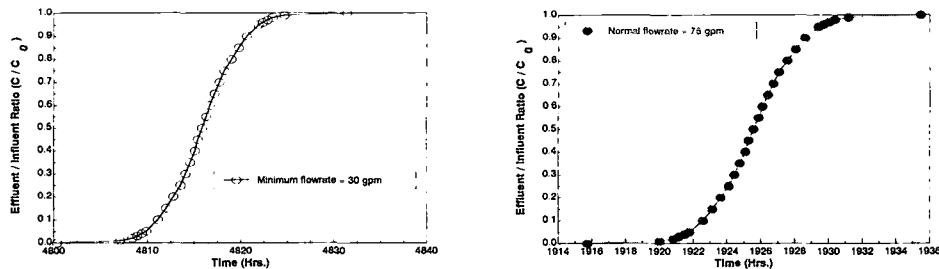


Fig. 2 Breakthrough curves for various letdown flowrates of PIX.

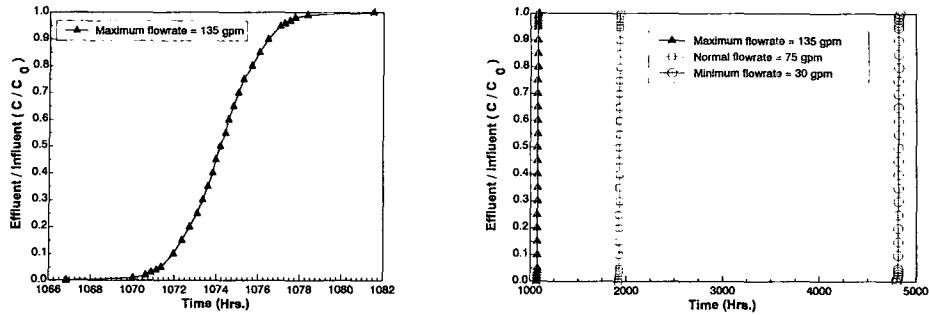


Fig. 2 Breakthrough curves for various letdown flowrates of PIX(Cont'd).

3-2-2. Effect of ion Exchange resin particle size

As the ion exchange resin particle size decreases from 1.2 mm to 0.55 and 0.2 mm, the slope of breakthrough curves for sulfate becomes steeper and the effluent breakthrough trace appears later as shown in Fig.3. This would be expected from the fact that the size of IX resin particle increases, the surface area and adsorption capacity are reduced. The effects of IX resin particle size on breakthrough curves are not significant as compared to that of the flowrate.

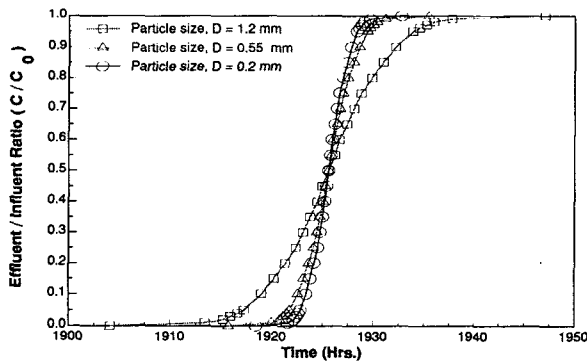


Fig. 3 Breakthrough curves for various resin particle sizes.
(Letdown flowrate = 75 gpm)

3-3 Breakthrough time and exhaustion time

When the effluent concentration reaches 5% of its value of the influent, the ion exchange zone is considered to reach the bottom of the PIX bed. The impurities start to efflute from PIX bed section for the first time. This is designated as the breakthrough

point. As the operation of the PIX column is continued, the concentration of effluent rises 95% of its value of the influent. At this point, the ion exchange zone is considered to reach the top of the PIX bed. The PIX is supposed to be completely exhausted. This is designated as the exhaustion point. As letdown flowrate increases from 30 gpm to 75 and 135 gpm, the times to reach the breakthrough point is reduced from 4,810 hr to 1,921 and 1,071 hr. As discussed above, the exhaustion time is also reduced from 4,822 hr to 1,930 and 1,077 hr. In case of normal letdown flowrate of 75 gpm, as the size of PIX resin particle is increased from 0.2 mm to 0.55 and 1.2 mm, the time to reach the breakthrough point is reduced from 1,923 hr to 1,921 and 1,917 hr and the exhaustion time is increased from 1,928 hr to 1,930 and 1,934 hr.

Table 2. Breakthrough time and Exhaustion time for PIX of UCN 3&4

Parameters	Max. flowrate 135 gpm, (D=0.55 mm)	Normal flowrate, 75 gpm			Min. flowrate 30 gpm, (D=0.55 mm)
		Particle, D =1.2 mm	Particle, D =0.55 mm	Particle, D =0.2 mm	
Breakthrough time, hr	1071	1917	1921	1923	4810
Exhaustion time, hr	1077	1934	1930	1928	4822

4. Conclusion

When the ion exchange resin particle size decreases, the slope of breakthrough curves for sulfate becomes steeper and the effluent breakthrough trace appears rapidly. While the size of IX resin particle increases, the surface area and adsorption capacity are reduced.

The effect of IX resin particle size on breakthrough curves are not significantly affected when compared to that of CVCS letdown flowrate.

As the CVCS letdown flowrate increases, the times to reach the breakthrough point and exhaustion point are reduced. In case of CVCS normal letdown flowrate for 75 gpm, as the size of PIX resin particle increases, the time to reach the breakthrough point is reduced and the exhaustion time is increased.

References

1. F.Helfferich, "Ion Exchange," McGraw-Hill, London, (1962).
2. G.E.Boyd, A.W.Adamson, and L.S.Meyers, *J.Amer.Chem.Soc.*, 69, 2836, (1947).
3. S.C.Foo and Richard G.Rice, "Sorption Equilibria and Rate Studies on Resinous Retardation Beads," *Ind.End.Chem.Fundam.*, 18(1), 68-75, (1979).
4. O.A.Hougen and W.R.Marshall, *Chem.Eng.Prog.*, 43, 197, (1947).
5. "Final Safety Analysis Report", Ulchin Nuclear Power Plant Units 3 & 4, Vol. 9, KEPCO.
6. "Amberlite Summary Chart Ion Exchange Resins Properties and Application," Catalog

- No., ALP 0206A/0788, 2nd Ed., Rohm and Haas Co., USA.
7. B.J.Hoffman and et al., "The Significance of Ion Exchange Equilibria and Kinetics in the Production of Ultrapure Water," 27th Annual Liberty Bell Corrosion Course, Philadelphia, Pennsylvania, October 11-13, (1989).
 8. Bocaraon, "Handbook of Chemistry and Physics 61st Edition," CRC Press, (1981), F-62
 9. A.Bilewicz and et al., "Sorption of radionuclides on inorganic ion exchange materials from high temperature water," *Water chemistry of nuclear reactor systems 5*, vol.2, BNES, London, (1989).